Article

Water Depth Variation Influence on the Mooring Line Design for FOWT within Shallow Water Region

Wei-Hua Huang [1] and Ray-Yeng Yang [2,*]

1   Department of Harbor Engineering, CECI Engineering Consultants, Inc., Taipei 11491, Taiwan; pigpig0506po@gmail.com
2   Department of Hydraulic and Ocean Engineering, National Cheng Kung University, Tainan 70101, Taiwan
*   Correspondence: ryyang@mail.ncku.edu.tw

Abstract: The objective of this paper was to present the modeling and optimization of mooring lines for floating offshore wind turbines (FOWT) located in various water depths from 50 m to 100 m in Taiwan western offshore areas. A semi-submersible floating wind turbine system is considered based on Offshore Code Comparison Collaborative Continuation (OC4) DeepCwind platform with the National Renewable Energy Laboratory (NREL) offshore 5-MW baseline wind turbine. The mooring lines proposed consist of a catenary mooring with studless chains. Three nominal sizes of the mooring chain links are taken into account with diameters of 95 mm, 115 mm and 135 mm. According to this configuration, a total of five mooring designs for different water depths (i.e., 50 m, 60 m, 70 m, 80 m, 100 m) are analyzed according to the rules and regulations of the two certification institutions, Det Norske Veritas (DNV) and American Petroleum Institute (API). Considering ultimate limit state (ULS), fatigue limit state (FLS) and maximum operating sea state (MOSS) based on a typhoon with a 50-year return period and current with a 10-year return period, 25-year design life, as well as 1-year return period, respectively, long-term predictions of breaking strength, fatigue and stability are performed. The software OrcaFlex version 10.3 d is used to simulate and design the mooring lines. The obtained results show that the shallow mooring design of 50 m water depth case presents the heaviest chains among the other water depths, increasing their mooring costs. On the other hand, the 100 m water design has much longer mooring lines, making this parameter the cost driving one. Thus, the minimum mooring cost range is from 60 m to 80 m water depth.

Keywords: FOWT; mooring line; water depth; semi-submersible; fatigue analysis; orcaflex

1. Introduction

The contractive effect of the Taiwan Strait enhances the wind speed of the northeast monsoon due to the geographical environment of the Central Mountain Range on Taiwan's island and the hills of southeastern China. On the west coast of Taiwan, the average wind speed can reach up to approximately 11.24 m per second measured at 100 m above sea level [1]. The abundance of offshore wind resources in Taiwan presents a significant opportunity for the offshore wind farm market. The Taiwanese government has certainly recognized the benefits of building an offshore wind market. In April 2018, the Bureau of Energy (BOE) in Taiwan held two rounds of offshore wind allocation to award seven companies an aggregate capacity of 3836 MW and completed the auction process two months later with an additional 1664 MW capacity. This total 5.5 GW capacity for the "Phase 2—Potential Sites Round" will come online between 2021 and 2025.

As the Taiwanese market moves into the "third zonal development round", much of the future potential exists in deeper water locations (>50 m depth) suitable for using floating wind turbines. However, in the Taiwan Strait, where the water depth is no more than 100 m, these water sites can increase fatigue loads and mooring footprints, to achieve the required restoring forces for catenary systems, resulting in larger and more expensive

mooring lines. Furthermore, Taiwan is located in a typhoon belt and has regular visits from violent wind forces. To officially develop FOWT (floating offshore wind turbines) in Taiwan, we need to not only design a reliable floating wind turbine system that can pass the International Electro-technical Commission (IEC) Class-T certification for typhoon-withstanding capability, but also optimize the mooring for different water depths, satisfying the requirements of mooring design codes to cope with the problems of the shallow water mooring challenge and these natural phenomena.

The purpose of this paper is to determine which parameters drive the mooring line design depending on five different water depths (50 m, 60 m, 70 m, 80 m, 100 m), choosing the optimal mooring configuration for the OC4-DeepCwind semi-submersible platform [2] according to the design rules and guidelines of the two certification bodies, DNV (Det Norske Veritas) [3] and API (American Petroleum Institute) [4].

They present two different mooring design criteria, including the minimum requirements for line tension and fatigue life analysis, which are mainly based on the "safety class" approach. If the mooring design satisfies these two ultimate and fatigue limit state criteria, the last step is to verify whether the pitch motion and offset of the floating platform are within an acceptable limit under the maximum operating sea state.

After conducting the engineering analysis and code check, a preliminary cost analysis is also performed and some recommendations are given to select the most suitable mooring design, as a function of water depth. The cost analysis of the study is only focused on the hardware costs of the mooring line, not including the installation costs. In addition, the overall weight is used to represent the mooring cost because mooring price is linearly related to weight in the market dealings.

There are a large number of variables required to be tuned during the mooring design process. Some parameters hence would be considered the same for all water depths to be able to compare the mooring designs and simplify the analysis, such as marine conditions, seabed profile, soil property, floating platform, wind turbine, anchor size, mooring material, and so on. Therefore, the mooring design would only depend on the length, weight and pre-tension of the lines.

1.1. Floating Platform and Wind Turbine

The considered FOWT model in this paper is based on OC4-DeepCwind semi-submersible floating platform and the NREL (National Renewable Energy Laboratory) offshore 5-MW baseline wind turbine. A schematic representation of the model is illustrated below in Figure 1. The platform geometry consists of a central main column serving as the foundation of the wind turbine as well as three offset columns that are arranged in a triangular array and connected to the main column through a series of smaller diameter pontoons and cross braces (see Figure 2). At the bases of the three offset columns are larger diameter cylinders which have the same effect as heave plates. They can help to suppress the motion, particularly in the heave direction, but also in roll and pitch, achieving the stability of the FOWT. Figure 3 presents the geometry and full-scale dimensions of the DeepCwind semi-submersible platform.

The wind turbine used for this study is a NREL offshore 5-MW baseline wind turbine [5], which is recognized as an industry-standard reference model that is representative of a typical utility-scale, multi-megawatt wind turbine. It takes the form of a conventional three-blade rotor, with variable-speed and variable blade-pitch control capabilities. Table 1 provides the properties of the NREL 5-MW baseline wind turbine.
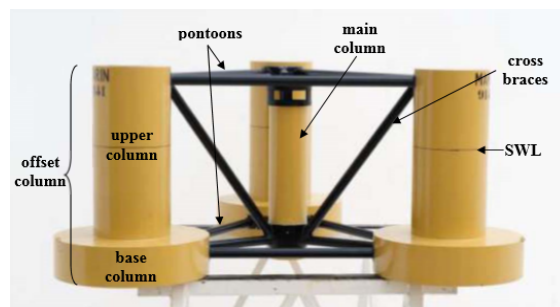
Figure 1. 3D view of the given OrcaFlex task.

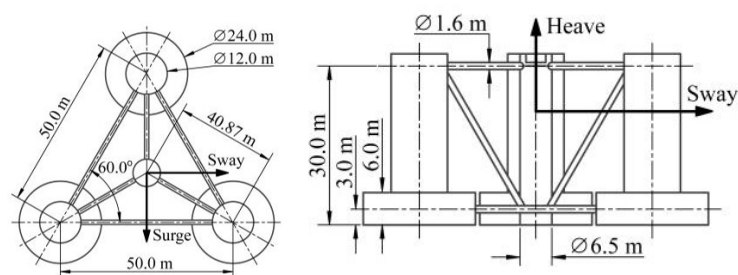**Figure 2.** As-built picture of DeepCwind semi-submersible for 1/50th scale tests [2].

Figure 3. Plan (**left**) and side (**right**) view of DeepCwind semi-submersible platform [2].

Table 1. Turbine characteristics [2].

NREL 5-MW Baseline Wind Turbine	
Rated power	5 MW
Rotor diameter	126 m
Hub height	90 m
Rated wind speed	11.4 m/s
Cut-in wind speed	3 m/s
Cut -off wind speed	25 m/s

1.2. Mooring Lines

Offshore moorings have been used for station-keeping of floating structures for a long time. The vital requirement for a mooring system is its ability to hold a floating structure or station under specific environmental conditions to allow various operations to be safely conducted.

There are three dominant mooring material types: chain, steel wire rope and synthetic fiber rope. Chain is the most common component used for the offshore operations. It is sturdy, durable and has a good resistance to seabed abrasion, as well as providing added holding capacity to the anchor. Thus in shallow waters, the "all-chain" design is extensively utilized. The mooring chain can be available in different types, diameters and grades depending on the application, fatigue considerations and strength demands.

The most common types of mooring configurations used for floating productions are the catenary and taut-leg. In catenary configuration, the mooring line can be divided in two parts, the suspended line which is connected to the floating foundation and freely hanging in the seawater. The other lies on the seabed segment that applies horizontal loads on the anchor. Figure 4 represents one catenary mooring line configuration.
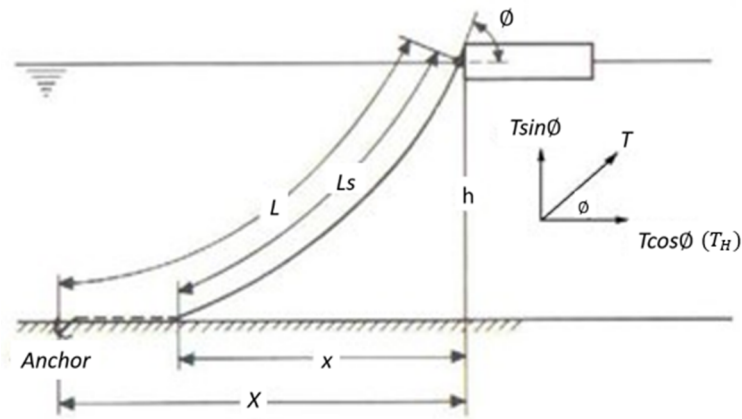

Figure 4. Catenary mooring arrangement.

Neglecting the hydrodynamic loads and assuming a single material in the elastic mooring line, the static catenary shape of suspended line can be written as Equation (1). Where water depth is h in [m], the mooring line wet weight per unit length is ω in [ton/m], the applied horizontal load to the mooring line at the fairlead is T_H in [ton] and the length of the suspended mooring line is L_s in [m] can be calculated with [6]:

$$L_s = h\sqrt{\left(2\frac{T_H}{\omega h} + 1\right)} \qquad (1)$$

The horizontal distance x between the fairlead and the touch down point of the mooring line on the seabed can be expressed as [6]:

$$x = \frac{T_H}{\omega}\cosh^{-1}\left(\frac{\omega h}{T_H} + 1\right) \qquad (2)$$

The distance between the anchor and the fairlead can be geometrically computed from:

$$X = L - L_s + x = L - L_s = h\sqrt{\left(2\frac{T_H}{\omega h} + 1\right)} + \frac{T_H}{\omega}\cosh^{-1}\left(\frac{\omega h}{T_H} + 1\right) \qquad (3)$$

Finally, in order to have the surge restoring line force, T_H is isolated from Equation (3) and derivate in [6]:

$$k_{11} = \frac{\partial T_H}{\partial X} = \omega \left[\frac{-2}{\left(2\frac{T_H}{\omega h} + 1\right)} + \cosh^{-1}\left(\frac{\omega h}{T_H} + 1\right) \right]^{-1} \qquad (4)$$

The catenary profile produces the geometric stiffness that is brought about by the weight of the mooring lines. The restoring force of the catenary system strongly depends on the weight of the mooring line, as it can observed in following Equation (4) [6].

1.3. Certification Requirements

The mooring design criteria typically define the minimum requirement for strength, fatigue life and floater offset in relation to the electrical cable design. Almost all of them use the dynamic analysis and safety class methodology to ensure the structure's and the mooring line's safety. In this study, DNV OS-E301 and API RP 2SK are used as a guideline and formulated in terms of three limit state equations to design the mooring lines of the FOWT. Definitions are given as follows:

1.3.1. Ultimate Limit State (ULS)

The ultimate limit state is to ensure that the individual mooring lines have adequate strength to withstand the load effect imposed by extreme environmental actions. The environmental effect for floating wind turbines is defined as a combination of wind and wave with 50-year return periods and current with a 10-year return period.

The design tension T_d in a mooring line constructed from two factored characteristic tension components is defined in Equation (5):

$$T_d = \gamma_{mean} \cdot T_{c,mean} + \gamma_{dyn} \cdot T_{c,dyn} \qquad (5)$$

The characteristic mean line tension $T_{c,mean}$ is defined as the mean part of the 50-year value of the line tension and is caused by pre-tension and mean environmental loads from dynamic wind, wave and current drift. The characteristic dynamic line tension $T_{c,dyn}$ is defined as the dynamic part of the 50-year value of the line tension and is induced by oscillatory low-frequency and wave-frequency motions. γ_{mean} and γ_{dyn} are load factors.

Then the characteristic strength of mooring line body can be obtained from the minimum breaking strength S_{mbs} of the mooring components as follows:

$$S_c = 0.95 \cdot S_{mbs} \qquad (6)$$

Finally, the design equation for the ULS is given by:

$$S_c > T_d \qquad (7)$$

where the characteristic quantities are defined above, and requirements for load factors are given in Table 2 as a function of safety class. The high safety class of the load factor is used for analysis in this paper.

Table 2. Load factor requirements for the ULS (ultimate limit state) [3].

Load Factor	Safety Class	
	Normal	**High**
γ_{mean}	1.3	1.5
γ_{dyn}	1.75	2.2

1.3.2. Fatigue Limit State (FLS)

Fatigue damage is a process of cycle-by-cycle accumulation of damage in a material undergoing fluctuating stresses and strains [7]. For calculating the fatigue damage due to the low frequency and wave frequency tension, the procedure consists of the following steps:

Step 1. Determine environmental conditions: A number of discrete bins to describe the environmental conditions are defined to represent the long-term environmental conditions.

Step 2. Determine the fatigue curve: This paper applies the T-N curve to calculate nominal tension fatigue lives of mooring components. It can be described by the following equation and should be obtained based on fatigue test data and a regression analysis.

$$NR^M = K \tag{8}$$

This equation may be linearized by taking logarithms to give:

$$\log(N) = \log(K) - M\log(R) \tag{9}$$

where N is number of permissible cycles corresponding to tension range ratio R, while R is the ratio of tension range (double amplitude) to RBS. M and K are slope and intercept of the T-N curves, respectively.

Step 3. Compute fatigue damage for each bin: When the tension time history is derived from the time domain analysis, the cycle counting method, such as the rainflow counting method can be adopted to obtain the tension variation cycles, and further to compute the annual fatigue damage for one environmental bin.

Step 4. Sum up the fatigue damage from all bins: After performing the rainflow counting, the annual cumulative fatigue damage can be calculated using Miner's rule:

$$D_c = \sum \frac{n_i}{N_i} \tag{10}$$

where n_i is number of cycles per year within the tension range interval *i*. N_i is the number of cycles to failure at normalized tension range *i* as given by the appropriate T-N curve.

According to Miner's rule, when the cumulative damage equals to 1, failure is predicted to have occurred. The fatigue design criteria is defined by:

$$D_c \cdot S_f \leq 1 \tag{11}$$

where S_f is the fatigue design safety factor. For permanent moorings, API fatigue approach recommends the safety factor of at least 3.0 should be applied. Note that some industry practices suggest increasing the safety factor from 3.0 to 10.0 for mooring components that are non-inspectable and in critical areas [8].

1.3.3. Maximum Operating Sea State (MOSS)

The MOSS (maximum operating sea state) load case is typically specified as a turbine operating during a 1-year return period typhoon. Under this defined condition, the thrust force is maximum at the rated wind speed, which makes it a design case. However, this thrust force applied at the hub height will generate a moment and platform inclination. To avoid the misalignment between the wind and the nacelle, inducing non-continuous power generation, the average pitch angle of the platform is required to remain at $\pm 1°$.

In addition, during operation, there may be other structures and facilities around the floating platform. To avoid damage on the platform and surroundings, the maximum offset allowance is imposed under this environmental loading, ensuring that floater motions remain within an acceptable limit. According to the API RP 2FP1, the maximum allowable offset for shallow water (below 300 feet, i.e., 91.44 m) flexible riser normally ranges from 15% to 25% of water depth.

2. Methodology

2.1. Time Domain Analysis Simulation

The simulation tool used in this paper is OrcaFlex [9]. OrcaFlex is a commercial simulation software developed by Orcina Ltd. that can perform dynamic analysis and design of offshore systems, typically including boundary conditions such as floating structures, vessels, buoys, etc., as well as finite element (FE) modelling of line structures. In addition to hydrodynamic loads, the software is capable of calculating the motion and forces acting on the platform and mooring line for all degrees of freedom at every time step. OrcaFlex version 10.3d is used for modelling and computations presented in this study.

2.2. Marine Data

The marine data depends on the site for location and water depth. In this study, the water depth of the selected offshore areas ranges from 50 to 100 m, and the offshore data are collected in Hsinchu offshore area of Taiwan, which is located at the red mark shown in Figure 5. However, the same environmental parameters are considered when analyzing and comparing the mooring designs for different water depths.
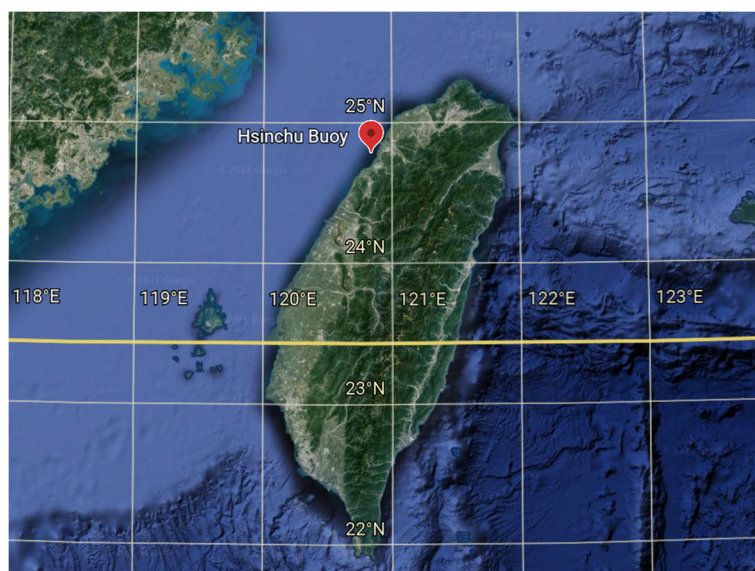

Figure 5. Location of the Hsinchu data buoy station.

In order to study the influence of water depth on FOWT mooring design, a simplified marine data set was defined in the attempt of representing the three main load cases: ULS, FLS (fatigue limit state) and MOSS. Their corresponding environmental conditions are as follows:

(1)   Ultimate Limit State

The wave environment considering a 50-year return period typhoon sea state is presented in Table 3. In this case, the wind velocity is considered as the IEC certification body which sets the class-T standard for typhoon-withstanding capability, rather than the 50-year return period wind speed. The class-T wind speed of 57 m per second at a reference height of 10 m is over the cut off speed and thus the turbine is parked.

(2)   Fatigue Limit State

From the year of 2005 to 2017, short term wave data measured for every hour were collected from the Coastal Ocean Monitoring Center (COMC). Seventeen short term sea states are produced with the two wave parameter increments of significant wave height and zero-crossing period, as seen in Table 4.

Table 3. Marine data for ULS load case.

Load Case	Turbine Condition	H$_s$(m)	T$_z$ (sec)	Wave Spectrum	Gamma	Wind Speed (m/s)	Current Speed (m/s)	Remark
		3 h Average				100 m above SWL	At Surface	
ULS	Parked	9.1	12.7	JONSWAP	2.08	57	1.16	50-year return period storm

Table 4. Wave scatter diagram for Hsinchu offshore area (%).

H$_s$ (m) / T$_s$ (s)	3.5	4.5	5.5	6.5	7.5	Sum
0.5	14.79	41.96	5.49	0.44	0.02	62.70
1.5	0.31	12.23	18.31	0.70	–	31.55
2.5	–	0.02	4.35	0.90	0.04	5.32
3.5	–	–	–	0.35	0.02	0.37
4.5	–	–	–	0.04	0.02	0.07
sum	15.10	54.21	28.16	2.43	0.11	100

Annual average current velocity and direction are presented in Table 5, where current direction was measured counter-clockwise based on northeastern direction as the zero degree. The measurement results of annual wind direction in the Hsinchu data buoy station reveal that wind from northeast appears most frequently, except for the summer season. Northeast wind presents high wind speed from late autumn to winter. Based on this statistic, the probability of occurrence was assumed to be 15%, 10%, 30%, 40% and 5% for Southwest (SW), North (N), North North-East (NNE), Northeast (NE) and East North-East (ENE). As mentioned above, in this paper, a 5-MW class wind turbine system will be considered with a rated wind speed 11.4 m/s. For conservative design, wind speed corresponding to the rated wind speed is applied instead of the actual wind speed. It is assumed that wind directions are same as the wave directions. Thus, five directions of wind and wave and two current directions yield ten load cases in total as shown in Table 5. Simultaneous consideration of short-term sea states with non-zero probability of occurrence in Table 4 and ten load cases in Table 5 produce 170 sub-load cases. Figure 6 presents a scheme of the wind, wave and current directions with reference to the floating wind turbine.

(3)   Maximum Operating Sea State

The MOSS load case covers a turbine operating during 1-year return period typhoon and its marine condition are shown in Table 6. The thrust force is maximum at the rated wind speed, which makes it a design case. The wind turbine NREL 5-MW has a rated wind speed at 11.4 m/s.

2.3. Design Process

This section explains the procedure that has been followed to design and optimize the mooring system for all water depths. The procedure is shown in Figure 7.

Table 5. Environmental bin according to current and wind conditions.

Bin	Current Dir (deg)	Current Speed (m/s)	Current Prob. of Occur (%)	Wind Dir (deg)	Wind Speed (m/s)	Wind Prob. of Occur (%)	Total (%)
1				180		15	11.25
2				45		10	7.5
3	22.5	0.93	75	22.5		30	22.5
4				0		40	30
5				−22.5	11.4	5	3.75
6				180		15	3.75
7				45		10	2.5
8	180	0.8	25	22.5		30	7.5
9				0		40	10
10				−22.5		5	1.25

Figure 6. Directions of environmental loadings.

Table 6. Marine data for MOSS (maximum operating sea state) load case.

Load Case	Turbine Condition	H_s (m) 3 h Average	T_z (sec) 3 h Average	Wave Spectrum	Gamma	Wind Speed (m/s) 100 m above SWL	Current Speed (m/s) At Surface	Remark
MOSS	Operating	3.58	8.79	JONSWAP	2.08	11.4	0.82	1-year return period storm

Input

Environment:	Floating structure:	Simulation tool:
- Water depth - Metocean conditions	- Geometry - Inertial properties (mass, center of gravity etc.)	Computation and design analysis software to be used

Mooring design

Configure mooring:
Mooring pattern, profile, number of lines, line lengths, size, fairlead coordinates and anchor locations.

Mooring system analysis

Generate mooring system modelling execute the mooring line ULS analysis

Does it satisfy the tension criteria — No

Yes

Mooring line FLS analysis

Does it satisfy the Fatigue damage criteria — No

Yes

Check platform stability results with MOSS load case

Does it satisfy platform Pitch and offset requirements — No

Yes

Final design of mooring system

Figure 7. Mooring design procedure of FOWT [6].

Having defined the FOWT's characteristics and expected the semi-submersible wind turbine to be deployed in the shallow waters with a depth of less than 100 m, the commonly used chain in shallow waters thus is selected as the studied mooring material. It is sturdy, durable and has a good resistance to seabed abrasion, as well as provides added holding capacity to the anchor.

For the mooring configuration, the catenary is the most commonly used system, especially in shallow to medium depth waters. The catenary profile produces the geometric stiffness that is brought about by the weight of the mooring lines. The weight of catenary

mooring contributes the position control of the floating platform. Therefore, in shallow waters, the "all-chain" design is extensively utilized.

After the mooring line material and configuration are decided, the size of the chain link should be determined for the given water depths. The size of the chain is defined by its nominal diameter. In this study, the three different nominal diameters of Grade R4 studless chain are taken into account: nominal diameters equal to 95 mm, 115 mm and 135 mm. The fundamental properties of the selected mooring chains are listed in Table 7.

Table 7. Characteristics of selected mooring line.

Nominal Diameter (m)	Proof Load (kN)	Break Load (kN)	Axial Stiffness (kN)	Unit Weight (ton/m)
0.095	6307.39	9001.17	770,735	0.1796
0.115	8836.42	12,610.30	112,942	0.2632
0.135	11,617.34	16,578.92	1,556,415	0.3627

As shown in Figure 8, the final selection of the mooring design consists of a 3×1 symmetrical spread of catenary mooring with studless chain. One of the lines is directed along the positive *x*-axis. The two remaining lines are distributed uniformly around the platform, such that each line is 120 degree apart when looking from above. The fairlead position is set to be located at the top of the base column.
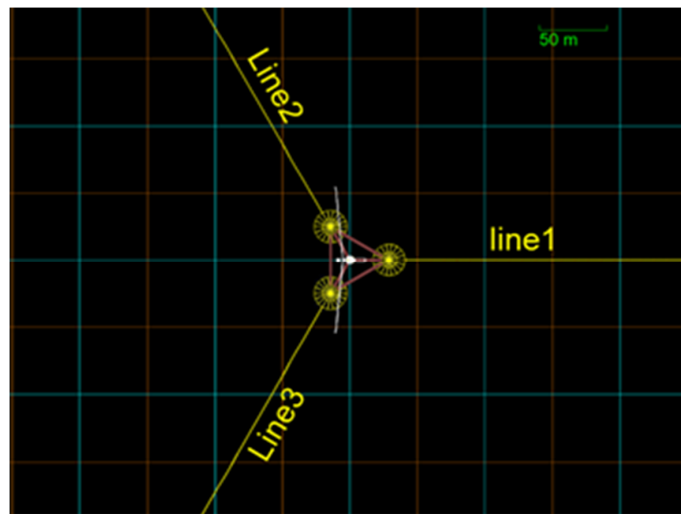
Figure 8. Mooring design arrangement.

After the length of the suspended mooring line is decided through the catenary equation. The long-term ultimate load case is iteratively conducted by increasing the ground chain length until the ultimate tension does not exceed the minimum breaking load of the mooring line.

Once the design of the heavy ground chain length is set, the fatigue strength should be checked in order to know whether the mooring design satisfies the fatigue life criteria or not. If the fatigue life of the mooring lines is not within the requirements for FLS load case, it should be return to first step "Mooring design" in Figure 7.

On the other hand, if the criteria parameters are satisfied, the last step is to verify whether the mooring design satisfies the criteria in the MOSS load case. If the platform pitch motion and offset meet its criteria, the final safety length of the mooring design is identified. On the other hand, if the pitch motion overpasses $\pm 1°$ or the offset criteria are not satisfied, the whole procedure would be repeated trying to increase the length of mooring line and therefore reducing the pitch motion and offset of the floating platform.

The final mooring system design is the one that satisfies all the criteria for all three load cases.

2.4. Assumptions

The mooring line design is strongly dependent on a large number of variables. Line pre-tensions, top angles, anchor tensions, maximum tensions, mooring lengths, mooring weights, mooring sizes, or mooring materials are some examples. As it has been explained in the previous chapter, the marine conditions, seabed profile, soil type, floating platform, wind turbine, anchor size and mooring material must be fixed for all cases. With the assumptions considered, the mooring design and optimization of the water depth specific mooring system is reduced to variations of:

(1)　The total length of the mooring chain;
(2)　The unit weight of the chain link;
(3)　The pre-tension of the mooring line.

3. Mooring Optimization Results and Discussion

Table 8 lists the final overall length of each nominal diameter mooring line for the different studied water depths. It can be seen that for a water depth range between 50 and 80 m the mooring line length increases linearly with the water depth. However, for water depths larger than 80 m, the trend of the line length seems to increase sharply.

Table 8. The final overall length of the mooring line (unit: m).

D	h	50	60	70	80	100
0.095		693.42	698.57	702.31	725.04	863.29
0.115		657.89	664.23	671.87	712.56	849.75
0.135		596.73	635.87	654.93	698.43	835.50

3.1. Verification of Ultimate Strength

Figure 9 presents the relationship of minimum breaking load (MBL) and design tension in accordance with the size of chain for each water depth. The MBL limit is shown in the Figure 9 as a dotted line. As it can be observed, for all three types of chain links, the design tension loads do not exceed the minimum breaking strength, and therefore the mooring designs meet the safety requirements imposed by the certification society in terms of ultimate design tensions.
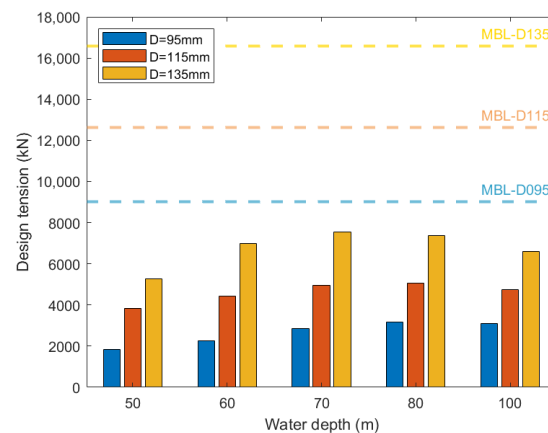
(**a**) Mooring line 1

Figure 9. *Cont.*
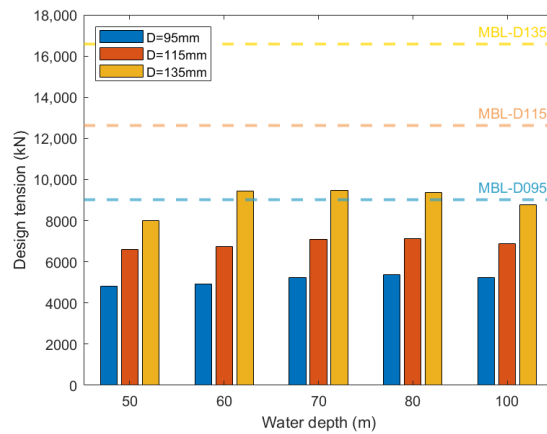
(**b**) Mooring line 2
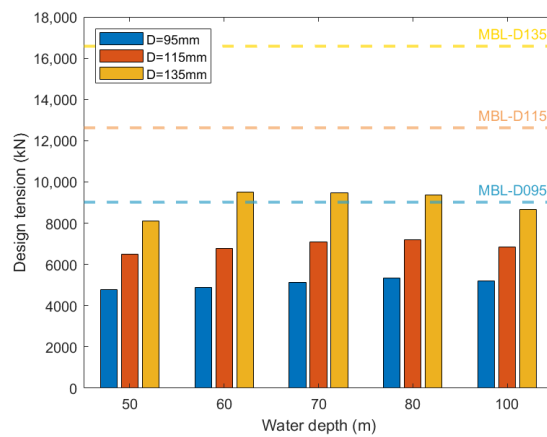
(**c**) Mooring line 3

Figure 9. Design tension of each mooring line for the different water depths.

3.2. Verification of Fatigue Strength

Figure 10 presents the cumulative fatigue damage considering the safety factor of 10.0 for three mooring lines. Since it is assumed that the fatigue fracture occurs only if the accumulative damage exceeds the unit value, the fatigue damage prediction suggests a much larger structure margin than the ultimate tension prediction in mooring line 2 and line 3.

3.3. Final Selection of Mooring System

After the mooring designs satisfaction of the limit state criteria in the ULS and FLS load case are verified, the results identify some trends of the mooring designs depending on the performance analysis. In this study, a new index of tension-fatigue product is proposed to evaluate the performance of the chosen mooring system. The tension-fatigue product, which is mainly based on the "safety class" approach and combined both ultimate and fatigue design criteria, can be determined using the following equation:

$$\text{Performance index} = \frac{T_d}{S_c} \times (D_c \cdot S_f) \tag{12}$$
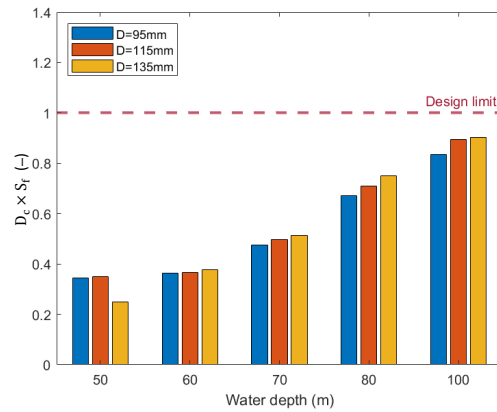
(**a**) Mooring line 1
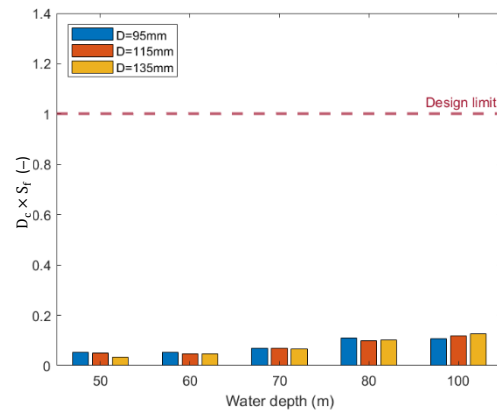
(**b**) Mooring line 2
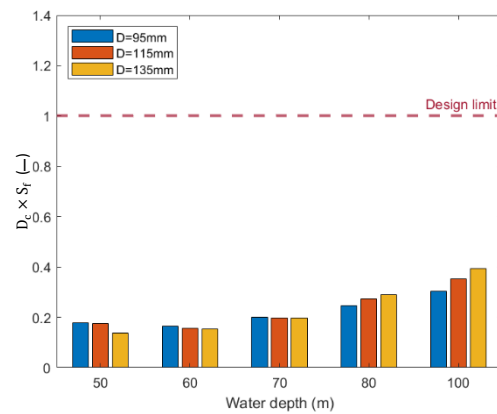
(**c**) Mooring line 3

**Figure 10.** Fatigue damage accumulated in each line for the different water depths.

The term in front of the multiplication represents the possibility of the mooring breaking under ULS load case and the term in parentheses indicates the possibility of the mooring failure under the FLS load case. Therefore, the smaller the tension-fatigue value is, the better the performance and more reliable the mooring design can be. Figure 11 presents the performance index value of each mooring line calculated through the previous analysis results.
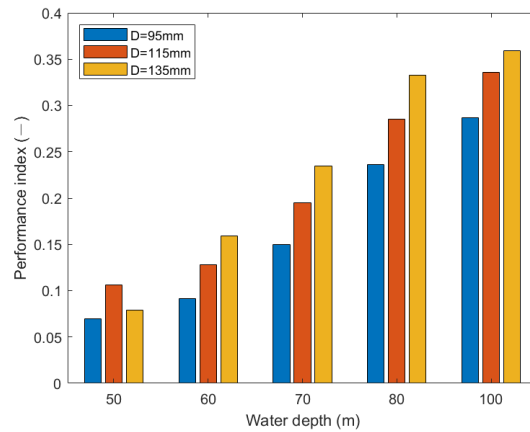
(**a**) Mooring line 1
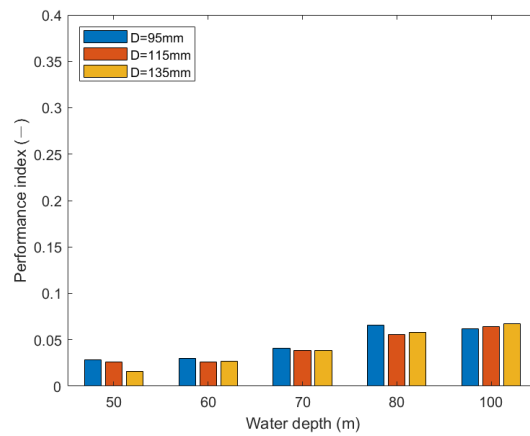
(**b**) Mooring line 2
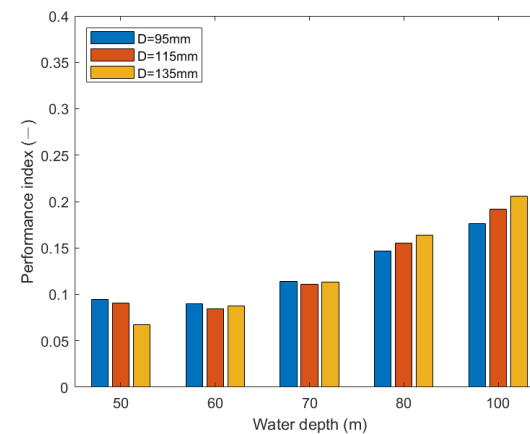
(**c**) Mooring line 3

Figure 11. Performance index value of each mooring line for the different water depths.

For the case of 50 m water depth, the design tension of D95 in mooring line 1 is relatively small, with the resulting minimum tension-fatigue values are shown in Figure 11. On the other hand, D135 would be the better choice in mooring line 2 and line 3. Using this method, the best options for the mooring system designs for the studied range of water depths are listed in Table 9.

Table 9. The final mooring system design for the studied water depth (unit: D (mm), L (m)).

Mooring	Water Depth	50 m	60 m	70 m	80 m	100 m
Line1		D95 L693	D95 L698	D95 L702	D95 L725	D95 L863
Line2		D135 L596	D115 L664	D115 L671	D115 L712	D115 L849
Line3		D135 L596	D115 L664	D115 L671	D115 L712	D95 L863

3.4. Verification of Maximum Operating Motion

Having determined the mooring system design for the studied water depths, the MOSS load case is carried out by applying the considered environmental conditions in order to check the results of the platform pitch motions and offsets. As it can be observed in Figure 12, there is no pitch motion response over the limit of $\pm 1°$, hence all the water depth cases satisfy the pitch motion criteria.

On the other hand, the platform's excursions decrease slightly with the water depth under the maximum design and operating condition. For the water case of 50 m, the maximum surge motions are measured between +2.5 m and −2 m, while the sway motions are restricted between +0.1 m and −0.9 m, that is to say, the maximum offset is well controlled within 5% of water depth. By contrast, for the water case of 100 m, the maximum surge motions are kept in ± 2 m and the sway motions are reduced by one third compared to the 50 m water case.

### 3.5. Mooring Hardware Cost Analysis

Finally, the hardware mooring costs of the FOWT are presented. The cost model refers to the market dealing algorithm of the mooring chain price, which is typically chain weight dependent. Therefore, the cost index in this study is presented as overall weight of the mooring line. It can be written as:

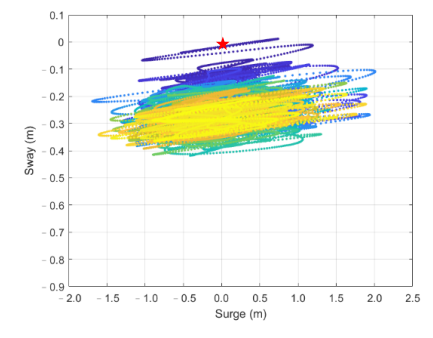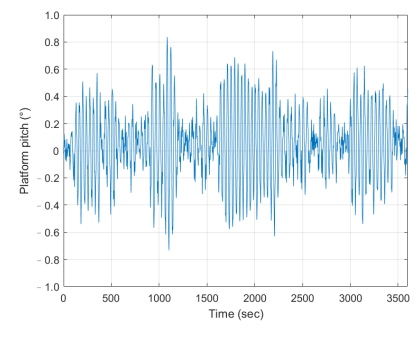$$\text{Cost index} = \text{unit weight} \times \text{overall length} \tag{13}$$

The cost indexes of each nominal diameter mooring line for five different water depths are listed in following Table 10.
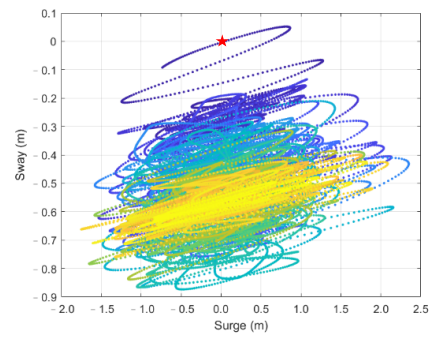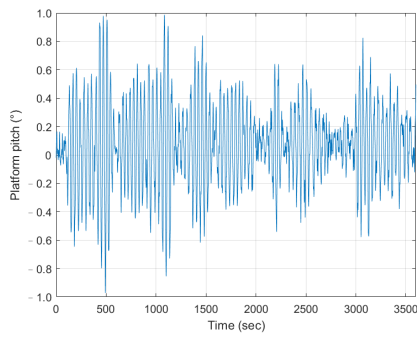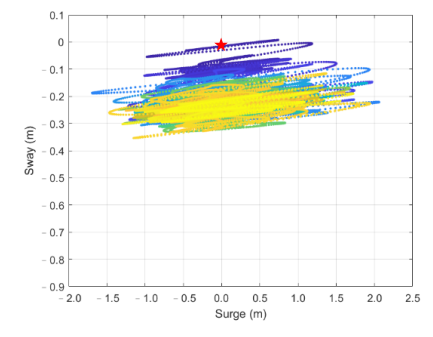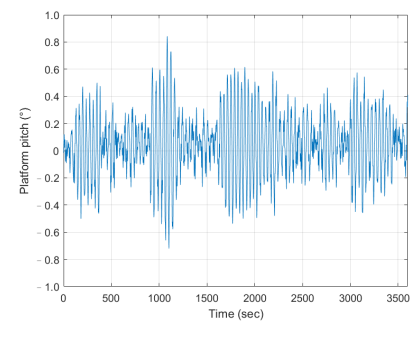
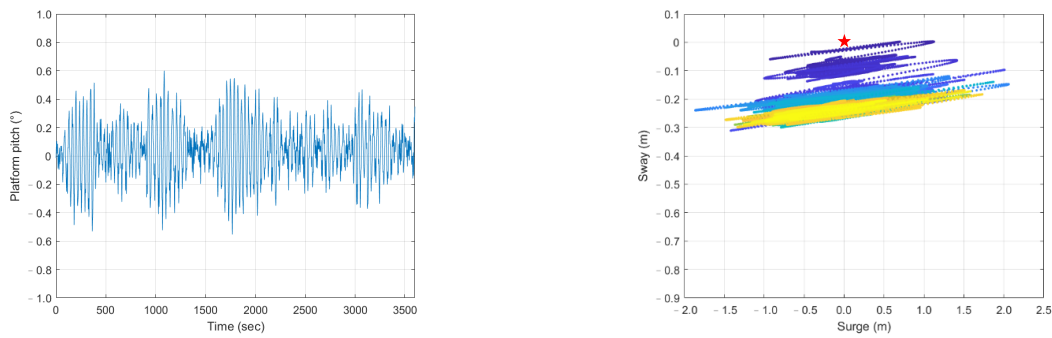(**a**) Water depth of 50 m.
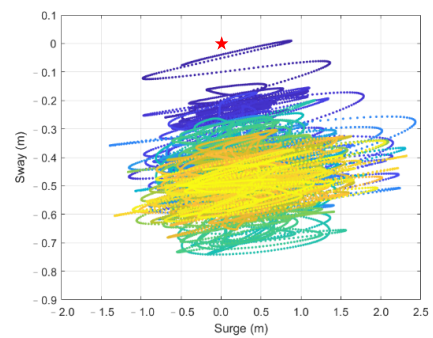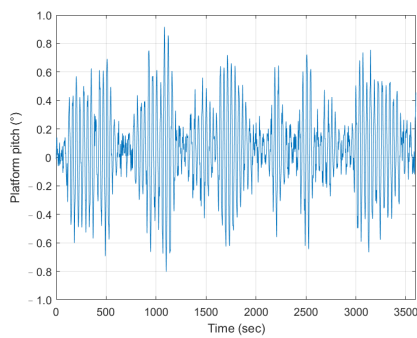
(**b**) Water depth of 60 m.

(**c**) Water depth of 70 m.

(**d**) Water depth of 80 m.

Figure 12. *Cont.*

(**e**) Water depth of 100 m.

Figure 12. Platform pitch motion (**left**) and offset (**right**) for the different water depths with wind, wave and current at $0°$.

Table 10. Value of cost index of each mooring line (unit: ton).

D (m)	H (m) 50	60	70	80	100
0.095	124.54	125.46	126.13	130.22	155.04
0.115	173.14	174.81	176.82	187.53	223.64
0.135	216.42	230.62	237.53	253.30	303.02

According to the previous mooring system design for each water depth, the total weight of the three mooring lines are summed up in Table 10. The results of the hardware mooring line costs for different water depths are presented in Figure 13.
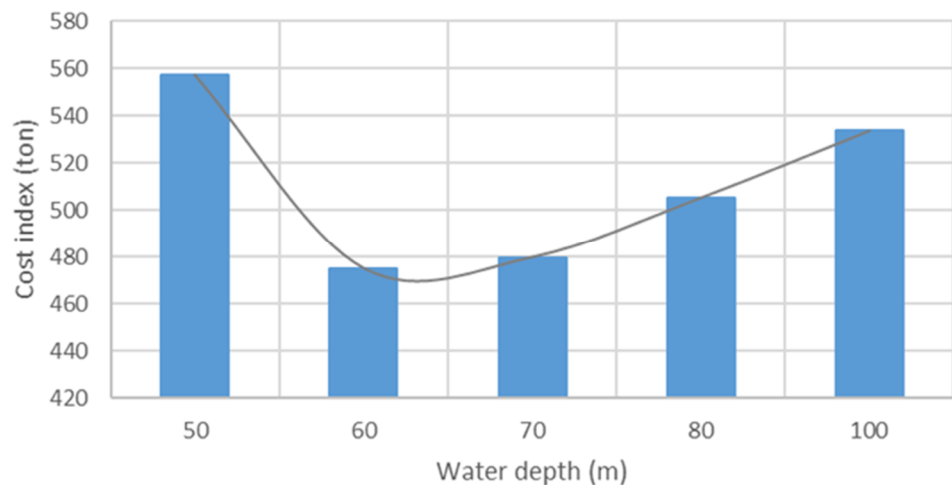

Figure 13. Hardware mooring cost for the different water depths.

The restoring capacity of a catenary system depends on the shape of the catenary, which requires higher gravity in shallow waters than deeper. This figure above presents the fact that shallow waters require a heavier chain to meet the requirements. When the water depth is less than 60 m, the mooring chain weight decreases exponentially as the water depth increases. The shallowest case of 50 m water depth has the heaviest chain. This fact makes the chain weight the driving parameter for designing the shallow water mooring lines, since slight decreases in water depth require heavier chains. However, this tendency continues until 60 m, where it reaches the lowest point.

On the other hand, when the water depth ranges between 60 m and 100 m, the mooring chain weight increases linearly with the water depth. The trend of the total costs has a minimum range from 60 m to 80 m water depth. This minimum is caused by two factors,

the mooring chain weight driving the costs of 50 m water case and the line length driving the costs of the 100 m water case.

4. Conclusions

This study presents and discusses five FOWT mooring system designs. These five mooring designs are divided into five different water depths: 50 m, 60 m, 70 m, 80 m and 100 m. The main objective was to identify the trends of the hardware mooring costs as the water depth variations.

The FOWT system typically consists of a wind turbine, floating platform and mooring system. The foundation is based on the OC4-DeepCwind Semisubmersible technology and the wind turbine uses the NREL 5-MW baseline turbine design. For the mooring system, the most feasible and reliable option for the studied water depths is a catenary configuration with an all-chain mooring system. Three nominal sizes of studless mooring chain links are taken into account: diameters of 95 mm, 115 mm and 135 mm.

In order to optimize and meet the standards of the certification bodies, the five designs have to satisfy specific criteria for three different load cases: ultimate limit state, fatigue limits state and maximum operating sea state load cases. For practical reasons, all designs have the same marine conditions, seabed profile, soil type, floating platform, wind turbine, anchor size and mooring material. Only three variables depend on water depth: the length, the weight and the pre-tension of the mooring line. The numerical software OrcaFlex version 10.3 d is used to simulate and design the mooring systems.

The design procedure of mooring lines for FOWT is explained in detail. Considering three marine conditions for all cases, the shallow mooring design of 50 m water depth presents the heaviest chains among the other water depths. Therefore, the heavy chain weight drives the design cost of 50 m waters. On the other hand, the 100 m water design has much longer mooring lines, making this parameter the cost driving one. This fact leads to a minimum range for the considered marine data from 60 m to 80 m water depth.

Institutional Review Board Statement: Not applicable.

Informed Consent Statement: Not applicable.

Data Availability Statement: Not applicable.

Conflicts of Interest: The authors declare no conflict of interest.

References

1. Chang, P.C.; Yang, R.Y.; Lai, C.M. Potential of offshore wind energy and extreme wind speed forecasting on the west coast of Taiwan. *Energies* **2015**, *8*, 1685–1700. [CrossRef]
2. Robertson, A.; Jonkman, J.; Masciola, M.; Goupee, A.; Coulling, A.; Luan, C. Definition of the Semisubmersible Floating System for Phase II of OC4. In Proceedings of the NREL/TP-5000-60601, National Renewable Energy Laboratory, Golden, CO, USA, 1 September 2014.
3. DNV. DNV-OS-E301: Position Mooring. Det Norske Veritas. 2010. Available online: https://rules.dnvgl.com/docs/pdf/DNV/codes/docs/2010-10/OS-E301.pdf (accessed on 12 April 2021).
4. American Petroleum Institute. *API Recommended Practice 2SK, Recommended Practice for Design and Analysis of Stationkeeping Systems for Floating Structures*, 3rd ed.; American Petroleum Institute: Washington, DC, USA, 2005; Addendum 2008, Reaffirmed 2015.
5. Jonkman, J.; Butterfield, S.; Musial, W.; Scott, G. *Definition of a 5-MW Reference Wind Turbine for Offshore System Development*; National Renewable Energy Lab. (NREL): Golden, CO, USA, 2009.

6. Ma, K.T.; Luo, Y.; Kwan, T.; Wu, Y. Mooring system engineering for offshore structures. In *Mooring System Engineering for Offshore Structures*; Elsevier: Amsterdam, The Netherlands, 2019.
7. Almar-Naess, A. *Fatigue Handbook: Offshore Steel Structures*; Tapir Academic Press: Trondheim, Norway, 1985.
8. ABS. *Guidance Notes on Certification of Offshore Mooring Chain*; American Bureau of Shipping: Houston, TX, USA, 2017; 55p.
9. Orcina Ltd. *OrcaFlex Version 10.3d*; Orcina Ltd.: Ulverston, UK, 2019.